An Extended Kalman Filter for Retained Volume Estimation in Peritoneal Perfusion Applications

Yejin Moon[1,*], Mahsa Doosthosseini[2,*], Behzad Kadkhodaeielyaderani[1,*], Joseph S. Friedberg[3,#], Jin-Oh Hahn[4,*], and Hosam K. Fathy[5,*,†]

***Abstract*— This paper develops and validates an extended Kalman filter for estimating the fluid volume retained in a patient's or a lab animal's peritoneal cavity during perfusion. Such estimation is potentially valuable for monitoring perfusion effectiveness and patient condition during medical interventions such as peritoneal dialysis. Monitoring intra-abdominal pressure and volume is particularly important for preventing undesirable or unsafe conditions such as intra-abdominal hypertension, abdominal compartment syndrome, etc. The literature already models the dynamics of peritoneal cavity pressure during perfusion. However, to the best of the authors' knowledge, the use of such models for online perfused volume estimation is a novel contribution of this paper. Specifically, the paper presents a simple model of cavity pressure dynamics, parameterizes it from a perfusion experiment on a large laboratory animal (namely, a Yorkshire swine), and uses it to design an extended Kalman filter for online retained volume estimation. The paper validates its approach by comparing the perfused volume estimate to a benchmark estimate generated using canister fluid level sensors embedded in the perfusion setup. The results of this validation are very encouraging, with 97% correlation between the two volume estimates.**

I. INTRODUCTION

This paper examines the problem of estimating the volume of fluid retained inside the peritoneal (i.e., abdominal) cavity of a patient or a laboratory animal during perfusion. At least two different perfusion applications have the potential to benefit from such online estimation. In the first application - namely, peritoneal dialysis - an aqueous solution is perfused (i.e., circulated) through a patient's abdominal cavity in order to absorb and ultimately remove toxins from the patient's bloodstream. In the second application, an oxygen-rich liquid, such as perfluorodecalin, is perfused through the abdomen in order to facilitate the diffusion of oxygen into the patient's or laboratory animal's bloodstream. Previous research suggests that such perfusion has the potential to enable the abdomen to serve as a "third lung," in a manner similar to its use as a "third kidney" during peritoneal dialysis [1]. This is important given the frequency of annual hospitalizations due to respiratory failure, especially during global emergencies such as the COVID-19 pandemic.

Fig. 1 is a high-level schematic of the perfusion setup used in this paper's research. The setup uses a peristaltic pump plus a suction canister to circulate oxygenated perfluorodecalin into and out of a laboratory animal's abdominal cavity, respectively. Carbon dioxide is purged from the perfusate, and oxygen is dissolved in it prior to perfusion. The setup has been employed for seven experiments on laboratory animals (specifically, Yorkshire swine) to date, with the ultimate goal of examining the effectiveness of this potential treatment.

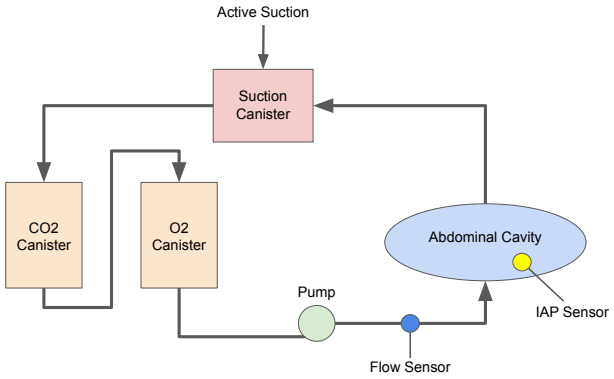

Fig. 1. Perfusion Setup

Regardless of the specific application, estimating the volume of fluid retained in the abdomen can be valuable for monitoring both the effectiveness and safety of perfusion. This is particularly important given the risk of intra-abdominal hypertension (IAH), characterized by a consistent increase in intra-abdominal pressure (IAP) beyond 12 $mmHg$ [2]. IAH can be caused by an excessive intra-abdominal volume (IAV), or "retained" volume in the abdomen [3]. If IAP values exceeding 20 $mmHg$ persist for a significant amount of time, patients can develop abdominal compartment syndrome (ACS). This can cause serious cardiovascular, respiratory, abdominal, neurological, or other adverse effects [2], [4]. Moreover, considering the high incidence of IAH among intensive care patients [5], [6], accurately measuring and characterizing the dynamics of IAP and IAV is extremely important during intensive care perfusion applications.

Different methods exist for measuring and monitoring IAP. Among these methods, the World Society of the Abdominal Compartment Syndrome recommends using trans-bladder pressure measurements in the strict supine position [2]. Although this monitoring approach is well-established, the fact remains that IAP varies significantly: *(i)* between different abdominal regions [7]; (ii) as a function of body positioning angle [8], [9], [10]; and *(iii)* as a result of conditions such as obesity, pregnancy, age, etc. [11], [12], [13], [14]. Moreover,

Author positions and affiliations: [1] Ph.D. student; [2] Postdoctoral fellow; [3] Thoracic surgeon-in-chief; [4] Associate Professor; [5] Professor; * Department of Mechanical Engineering, The University of Maryland, College Park; # Lewis Katz School of Medicine at Temple University; † Corresponding author (hfathy@umd.edu).

abdominal cavity compliance can change from one patient to another for reasons including prior surgeries [15]. Finally, the effectiveness of perfusion applications such as peritoneal dialysis depends heavily on choosing the correct fill volumes adapted to each patient [16]. Altogether, the above factors highlight the importance of monitoring both IAP and IAV. The main goal of this paper is to enable such online volume estimation as an additional capability that complements online IAP measurement.

At least four approaches can be used for estimating IAV, each having its strengths and limitations. First, one can estimate IAV by measuring perfusion inflow and outflow, then integrating the difference between these two flowrates. This method suffers from the inevitable drift inaccuracies associated with integration of flowrate measurement bias. Second, one can equip the patient bed with weight sensors, then attribute changes in test animal or patient weight to changes in IAV. This approach can falsely construe other added weights (e.g., new sensors mounted on the patient bed) as reflecting changes in IAV. Third, one can use level sensors to measure the fluid remaining inside the perfusion setup's canisters, then attribute changes in these measurements to perfusion. This is reasonable for short perfusion experiments with negligible fluid leakage and/or evaporation: a fact that justifies its use as a benchmark in this paper. Finally, one can use feedback observers to estimate retained volume from perfusate flowrate and IAP measurements. Feedback estimation allows this approach to be potentially robust to the slow loss of fluid due to evaporation and/or leakage: a key advantage that motivates its adoption in this work.

The literature already examines the relationship between IAV and IAP for both humans and other mammals [8], [9]. Some studies approximate this relationship as affine [8], [9], [17], [18], with more recent studies emphasizing the nonlinear nature of this relationship for higher IAV/IAP values (e.g., IAP $> 15\ mmHg$) [4], [19]. In particular, as IAV increases, there is first a small drop in incremental peritoneal cavity stiffness, followed by nearly exponential stiffening for higher values of IAV/IAP. The above studies are useful because the dynamic relationship between IAV and IAP can serve as a plant model for online IAV estimation. To the best of the authors' knowledge, the novelty of this work stems from the fact that it builds on the above literature to both propose and experimentally validates a feedback-based online perfused volume estimator, for the first time. The estimator assumes that both IAP and perfusate inflow rates are measured experimentally, then uses an extended Kalman filter (EKF) for online IAV estimation.

The remainder of this paper is organized as follows. Section II describes the perfusion setup used in this study's animal experiment. Section III presents the state-space model used for representing cavity pressure dynamics, as well as the outcomes of fitting this model to animal experiment data. Section IV presents the approach used for designing the perfused volume estimator, as well as the performance of this IAV estimator. Finally, Section V summarizes the paper's conclusions.

II. EXPERIMENTAL SETUP

The motivating application for this work is the peritoneal perfusion of oxygenated perfluorocarbons. Perfluorocarbons (PFCs) are compounds consisting of carbon chains or rings covalently bonded to fluorine. The characteristics of the carbon-fluorine bond allow PFCs to dissolve unusually high amounts of both oxygen and carbon dioxide [20], [21], [22], [23]. This has motivated research on the use of the peritoneal perfusion of oxygenated PFCs to provide a potential pathway for the diffusion-based transport of oxygen into test animals' bloodstreams [1]. The resulting "third lung" intervention is potentially appealing as a treatment for patients experiencing respiratory failure due to acute respiratory distress syndrome (ARDS), COVID-19, etc.

Fig. 1 provides a high-level sketch of the setup used in this paper, with additional details appearing in a companion article [24]. The setup uses a peristaltic pump to supply PFC into lab animals' abdominal cavities. A cis-\trans-perfluorodecalin mix is supplied to and drained from the test animals through 36 French (i.e., $12mm$ diameter) venous cannulas terminating in foam-covered custom diffusers. PFC drainage is facilitated via active suction provided by a manually-controlled vacuum pump. The setup contains three canisters: a CO2 removal canister, an oxygenation canister, and a suction canister. A pressure sensor is mounted at the top of the suction canister and used for measuring negative suction pressure. Furthermore, to measure the level of PFC in each canister, additional pressure sensors are mounted at the bottoms of the three canisters. The setup measures PFC inflow into the animal using a flowrate sensor. Moreover, the setup's data acquisition system monitors the signals from three catheter-mounted sensors for measuring IAP, bladder pressure, and inferior vena cava pressure.

Seven IACUC-approved animal experiments have been performed to date on the "third lung" concept using the above setup. The work in this paper focuses on the seventh animal experiment due to the availability of a reliable benchmark measurement of perfused volume from this experiment's dataset. Perfusion was performed on an adult Yorkshire swine, anesthetized for the full duration of the experiment. The experiment provided two estimates of perfused volume versus time, using two separate sets of sensors, namely: an IAV estimate using the proposed EKF algorithm, plus a benchmark estimate utilizing the pressure-based canister level sensors. As shown in the remainder of this paper, the strong linear correlation between these two estimates serves as a validation of the proposed EKF concept.

III. CAVITY PRESSURE DYNAMICS AND SYSTEM IDENTIFICATION

This section introduces a simple first-order nonlinear state-space model of cavity pressure dynamics. This model serves as the open-loop predictor component of the proposed EKF algorithm. The two inputs to this model are the volumetric PFC flowrate (measured by the perfusion flowrate sensor) and the ambient suction pressure (measured by the pressure sensor mounted at the top of the suction canister). The output

of the model is IAP, and the state variable is IAV. Thus, the availability of physical IAP measurements enables the use of feedback-based IAV state estimation in conjunction with this model. All pressure measurements presented in this paper are gauge pressures. Hence a pressure reading of zero indicates atmospheric conditions. The equations below summarize the proposed state-space model for the cavity dynamics.

$$\begin{aligned} \frac{dV(t)}{dt} &= Q_{in}(t) - Q_{out}(t) = Q_{in}(t) - C_o \delta P(t) \\ P(t) &= \beta_1 V(t) + \beta_2 V(t)^2 + \beta_3 V(t)^3 \\ \delta P(t) &= P(t) - C_\infty P_\infty \\ V(0) &= V_o \end{aligned} \tag{1}$$

The variables and parameters in the above equations are defined below with their dimensions.

$P(t)$	= Peritoneal intra-cavity pressure, IAP $(mmHg)$
$V(t)$	= Peritoneal intra-cavity volume, IAV (L)
V_o	= Initial intra-cavity volume (L)
$Q_{in}(t)$	= PFC inflow (L/min)
$Q_{out}(t)$	= PFC outflow (L/min)
$P_\infty(t)$	= Ambient pressure $(mmHg)$
$\delta P(t)$	= Drainage pressure difference $(mmHg)$
C_o	= Discharge constant $(L/min/mmHg)$
C_∞	= Ambient pressure coefficient
β_i	= P-V relationship coefficients $(mmHg/L^i)$

This state-space model uses a cubic relationship between the IAV, $V(t)$, and the IAP, $P(t)$, characterized by three unknown constants, β_1, β_2, and β_3. The rate of change of $V(t)$, $dV(t)/dt$ is the difference between PFC inflow and outflow, where PFC outflow is a product of a linear discharge coefficient, C_o, and the drainage pressure difference, δP. The model can be applied to different datasets, including datasets that begin after the initiation of perfusion. Hence, the possibility of a non-zero initial volume of PFC is recognized by setting $V(0) = V_o$ for some unknown, potentially non-zero, V_o. Drainage pressure difference, δP, is defined as the difference between $P(t)$ and the product $C_\infty P_\infty$ of an ambient pressure coefficient C_∞ and ambient pressure P_∞. Here, the ambient pressure coefficient represents the fact that the full extent of the negative ambient pressure, P_∞, measured at the top of the suction canister, may not be felt at the animal's discharge port due to simple factors such as air leakage in the suction canister.

Using Eq. (1), system identification was performed to estimate V_o, C_o, C_∞, β_1, β_2, and β_3. Approximately 370 seconds of the seventh experimental perfusion dataset were used to fit the model. The system identification objective was minimizing the summed square cavity pressure prediction error over the selected time horizon, subject to the proposed cavity dynamics model Eq. (1) as a constraint. Optimization was done using Matlab's particle swarm algorithm with a time step $\delta t = 10$ seconds.

Fig. 2 and Fig. 3 show the two inputs to the state-space model, PFC perfusion flowrate and ambient suction pressure, respectively. These two signals were filtered using a moving average filter applied over a 10-second window. At the beginning of the experiment, a perfusion flowrate reaching approximately 4 liters per minute is applied intermittently until the 75- second mark. Then, a steady flowrate of approximately 2.5 liters per minute is applied between the 75- and 300- second marks. Perfusion was stopped afterwards, leading to a zero flowrate. A relatively consistent small suction pressure between approximately $-8mmHg$ and $-2mmHg$ was applied throughout this experiment. As a result, cavity pressure decreases gradually over time, as seen in Fig. 4, due to the rapid termination of perfusion plus the steady application of mild active suction.

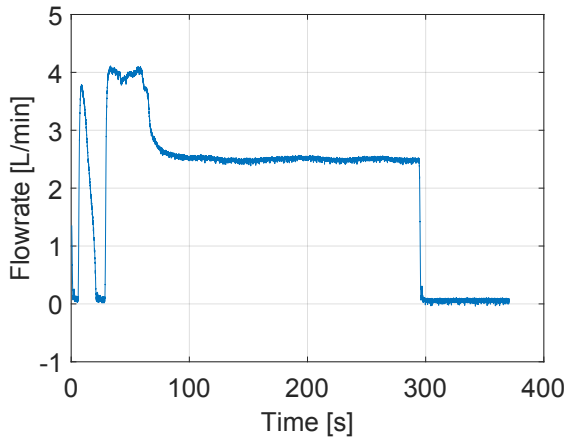

Fig. 2. PFC perfusion flowrate

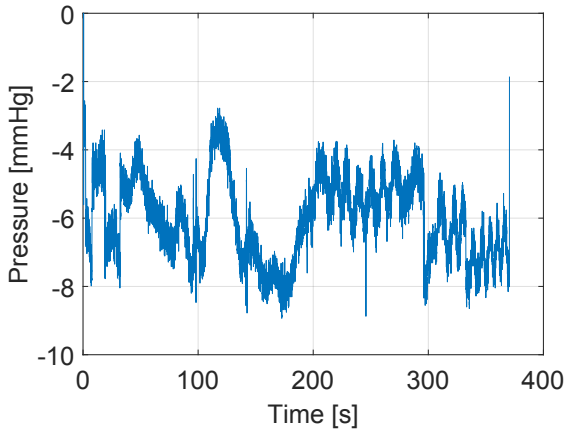

Fig. 3. Ambient suction pressure

Fig. 4 compares the measured and (optimal) estimated cavity pressure profiles for this time window. One interesting observation is that the measured IAP follows a staircase pattern, whereas estimated IAP is much smoother versus time. The staircase pattern of IAP measurement suggests either a pulsating outflow from the animal or the intermittent blockage of the IAP measurement catheter inside the test animal. Plots of bladder and vena cava pressure versus time, omitted for brevity, do not exhibit a staircase pattern. This

strongly suggests that the staircase pattern is likely caused by intermittent measurement catheter blockage. The fact that the estimated pressure signal tracks the general trend of measured IAP is, therefore, an encouraging indication of a reasonable model fit. Fig. 5 and Fig. 6 show that the residuals associated with this fit are reasonable, both as a function of time and in terms of their statistical distribution. Finally, Fig. 7 plots the auto-correlation of these residuals, for a 10-second time lag. The fact that these residuals are not white suggests the presence of unmodeled effects, most likely associated with the intermittent blockage of the IAP measurement catheter.

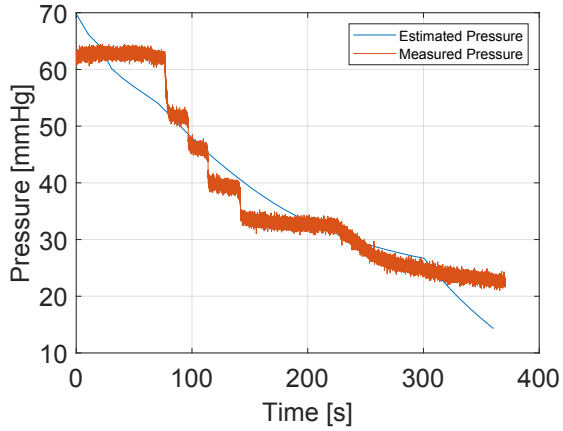

Fig. 4. Estimated cavity pressure and measured cavity pressure

The above system identification results correspond to the following optimal parameter estimates: $C_\infty = 0.2$, $V_o = 15L$, $C_o = 0.1062(L/min)/mmHg$, $\beta_1 = 6.0153 mmHg/L$, $\beta_2 = -0.0916 mmHg/(L^2)$, and $\beta_3 = 0 mmHg/(L^3)$. Among these parameters, β_1, β_2, and C_o are interior optima. These parameters correspond to a linear cavity discharge law and a weakly quadratic pressure-volume relationship, as shown in Fig. 8 and Fig. 9, respectively. The

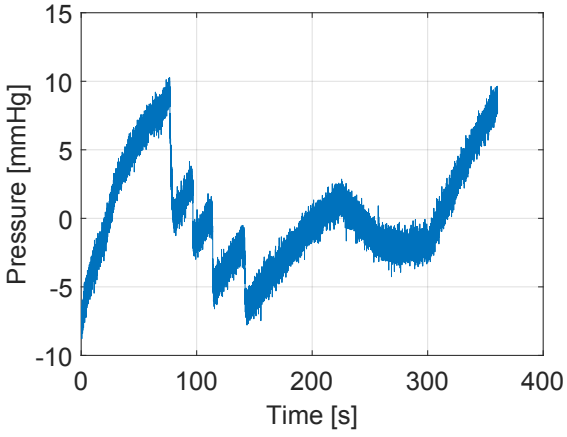

Fig. 5. Cavity pressure prediction residuals

quadratic term in the pressure-volume relationship suggests a slight reduction in incremental abdominal cavity stiffness with increasing IAV. This phenomenon has been observed in the literature for intermediate IAV values, and is typically followed by abrupt cavity stiffening at higher IAV values.

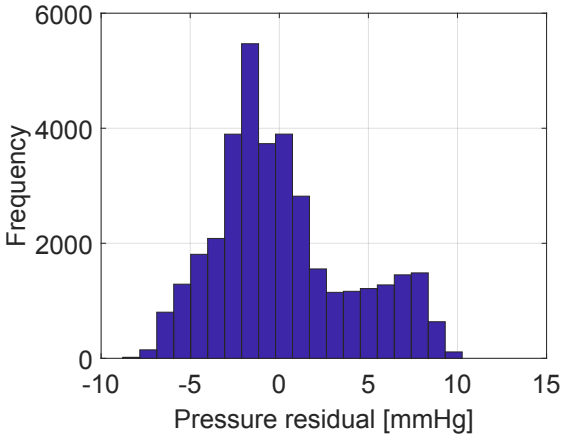

Fig. 6. Histogram of cavity pressure prediction residuals

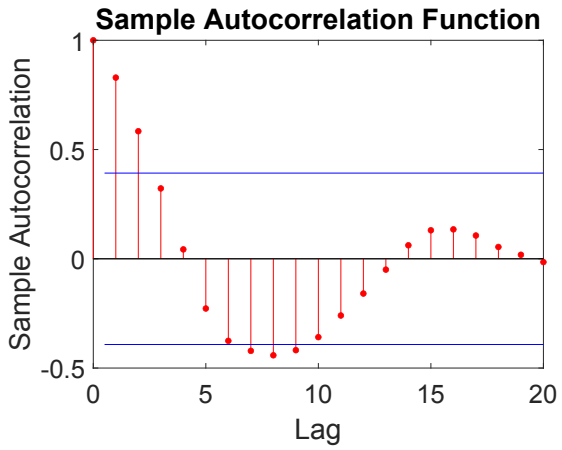

Fig. 7. Auto-correlation of cavity pressure residuals

The degree to which the above model can predict IAV is critical for its successful use in extended Kalman filtering. With this in mind, the optimal estimated IAV and the change of the volume of PFC in the perfusion setup were compared during the above time horizon. To compute the change of the volume of PFC in the setup, the pressure sensors mounted at the bottoms of the CO2, O2, and suction canisters were used to compute the level of PFC inside each canister, which ultimately enabled the computation of the total volume of PFC in each canister. Then, the volume of PFC in all canisters was combined to get the total volume of PFC in the setup, which was subtracted from the initial PFC volume to calculate the PFC volume change over time. The estimated IAV and the PFC volume change in the setup are both shown in Fig. 10. The two signals are shifted vertically relative to

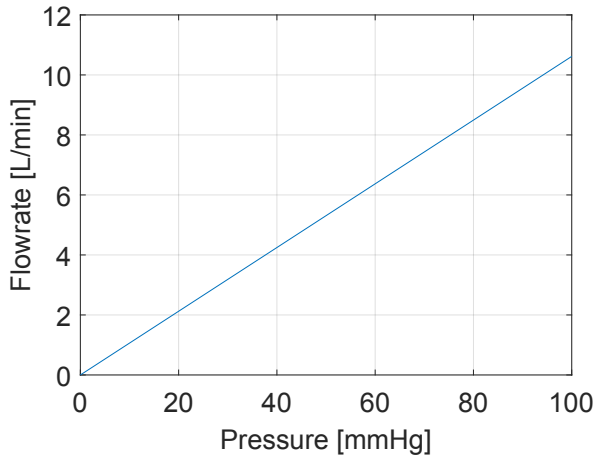

Fig. 8. Estimated cavity discharge characteristics

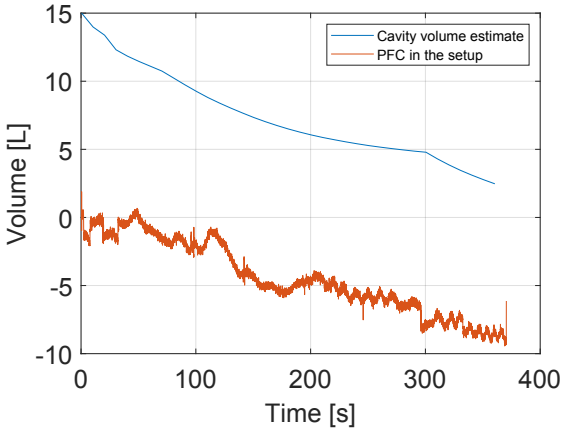

Fig. 10. Estimated perfused PFC volume

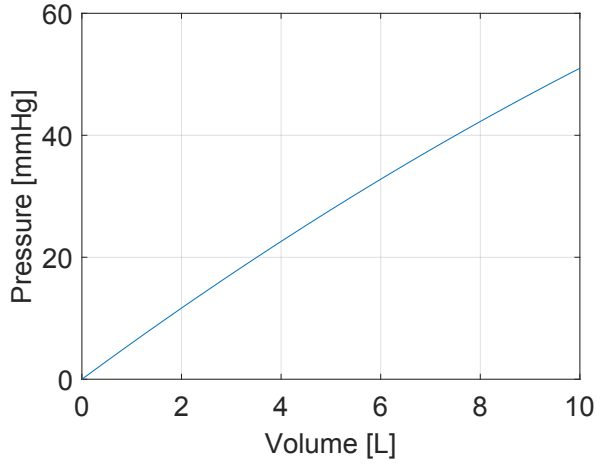

Fig. 9. Estimated cavity pressure-volume characteristics

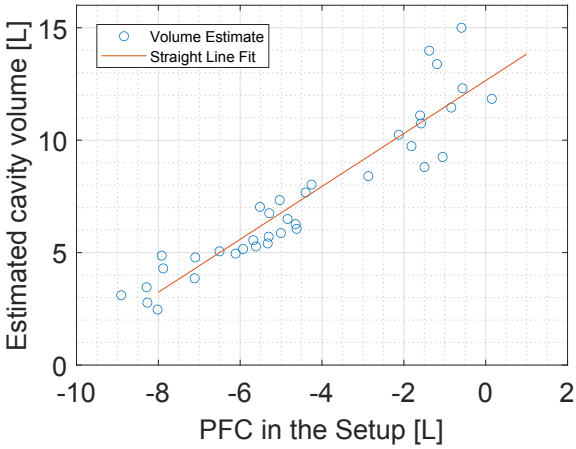

Fig. 11. Linear Regression

each other. This makes sense, considering the fact that one of the two signals is an estimate of *absolute* retained fluid volume whereas the other signal is an estimate of *change* in PFC volume inside the setup's canisters.

The two volume estimates in Fig. 10 are obtained using two separate estimation methods and, more importantly, two separate sets of sensors. This suggests that if one of these estimates - namely, the estimate obtained using the canister level sensors - is treated as a benchmark, a strong correlation between the two estimates can provide confidence in the second estimate. Fig. 11 pursues this validation exercise by plotting the level sensor-based estimate of PFC in the setup on the x-axis versus the estimated retained PFC volume on the y-axis. Both signals are sampled at a rate of 1 sample every 10 seconds in order to ensure consistency with the simulation model's 10-second time step. A strong linear correlation is visible between the two signals, with the red line in Fig. 11 indicating the best straight line fit for this correlation. The slope of the straight line fit is 1.17, meaning that when the volume of PFC in the setup's canister experiences an estimated change of $1L$, perfused volume experiences an estimated change of $1.17L$. This makes intuitive sense, given the difference between the two volumes being estimated and the fact that the experiment under consideration mostly involves fluid drainage from the lab animal. Specifically, as the animal is drained of PFC, a portion of the drained fluid fills the outflow catheter as opposed to the perfusion setup's canisters, potentially explaining the above discrepancy. Perhaps most importantly, the coefficient of determination (or "R-squared" value) associated with this straight-line correlation is 0.97, suggesting that 97% of the variations in the above two volume estimates can be explained through this linear correlation. This serves as a strong validation of the degree to which the proposed pressure dynamics model - while simple - can serve as a foundation for online perfused volume estimation.

IV. DESIGN AND VALIDATION OF EKF-BASED PERFUSED VOLUME ESTIMATOR

The perfused (or retained) volume estimate in Fig. 10 reflects the open-loop simulation of an optimally parameterized cavity pressure dynamics model. In other words, it reflects an open-loop estimate of IAV for an optimized initial condition. For online applications, one alternative to finding the optimal initial condition of the volume estimate is to use a feedback estimator. In this work, considering the nonlinearity of the pressure-volume relationship in Eq. 1, we use an extended Kalman filter (EKF) for perfused volume estimation. The governing equations for this EKF are:

$$\begin{aligned} \frac{d\hat{V}(t)}{dt} &= Q_{in}(t) - C_o\delta\hat{P}(t) + K(t)[P(t) - \hat{P}(t)] \\ \delta\hat{P}(t) &= \hat{P}(t) - C_\infty P_\infty \\ \hat{P}(t) &= \beta_1\hat{V}(t) + \beta_2\hat{V}(t)^2 + \beta_3\hat{V}(t)^3 \end{aligned} \tag{2}$$

In the above equation, $\hat{V}(t)$ and $\hat{P}(t)$ are the EKF-based estimates of IAV and IAP, respectively. The term $K(t)$ is a time-varying Kalman gain, computed by applying the Algebraic Ricatti Equation to a local linearization of the governing cavity pressure dynamics model around the current perfused volume estimate, $\hat{V}(t)$. In solving this Ricatti equation, we tune the filtering algorithm by setting the process noise variance to $\mathcal{W} = 2.5 \times 10^{-3} L^2 s^{-2}$ and the sensor noise variance to $\mathcal{V} = 0.25 mmHg^2$. As in the open-loop cavity pressure dynamics model, the terms $Q_{in}(t)$ and $P_\infty(t)$ represent the sensor measurements of the perfusate's inflow rate and ambient pressure, respectively. Moreover, the term $P(t)$ represents the experimentally measured IAP.

The basic idea behind the proposed EKF algorithm can be summarized as follows. The algorithm assumes that the flowrate of PFC into the abdominal cavity and the ambient suction pressure are measured. Using the cavity pressure dynamics model, and assuming this model to be accurate, the EKF algorithm predicts the rate of change of perfused volume versus time. It then corrects this prediction by feeding back the error between measured and predicted IAP, with the Kalman gain serving as a time-varying correction multiplier. The end result is a classical nonlinear estimator that employs feedback to both correct its estimates and pursues some degree of potential robustness to modeling errors.

Fig. 12 compares the measured IAP from the experimental data versus the predicted pressure using the EKF. The EKF's perfused volume estimate is initially set to $1L$ to generate this figure. As shown in the plot, the predicted pressure converges with the pressure measurement data after approximately 50 seconds. During the rest of the time horizon, the EKF tracks the measured pressure signal quite accurately. Fig. 13 compares the predicted volume from the EKF to: *(i)* the perfused volume estimate obtained by applying the linear regression formula from the previous section to the canister volume estimate; and *(ii)* the open-loop perfused volume estimate obtained from system identification. As depicted

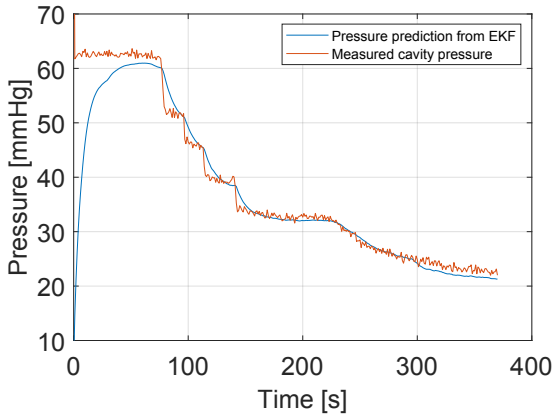

Fig. 12. Measured cavity pressure and estimated pressure via EKF

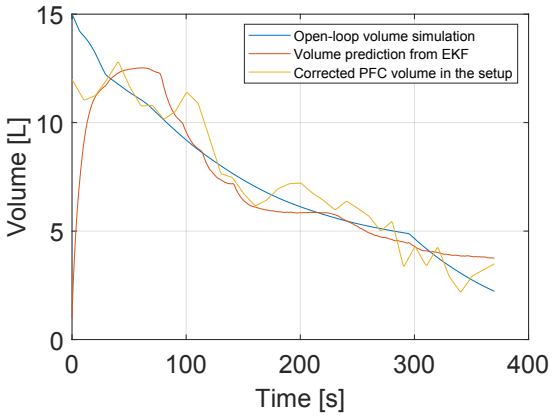

Fig. 13. Open-loop volume simulation, estimated volume via EKF, and measured PFC volume in the setup

in the figure, the EKF volume signal converges with the remaining curves in approximately 50 seconds. Then, during the rest of the time horizon, all three graphs decrease from 10 L to 2.5 L, closely following each other. This demonstrates the success of the proposed EKF algorithm in estimating IAP and (more importantly) IAV based on the modeled cavity pressure dynamics.

V. CONCLUSIONS

This paper models the dynamics of peritoneal intra-cavity pressure in a laboratory pig and uses this state-space model to design a perfused volume estimator using EKF. A good fit was obtained between the experimental data, open-loop simulation, and the EKF model. This shows that the EKF algorithm, employing the cavity pressure dynamics model, can indeed accurately estimate IAP and IAV. The novelty of the work stems from its development and validation of the EKF as an online algorithm for perfused volume estimation. Future work will examine the problem of applying this approach across multiple experimental settings and animals, perhaps in an adaptive manner that accounts for animal-

to-animal variability in underlying pressure dynamics. Such an extended application of this work is valuable both for validation and maximizing the richness of the datasets used in model parameterization and EKF algorithm development.

ACKNOWLEDGMENTS

The research in this paper was conducted under IACUC #0121006 at The University of Maryland Medical School, Baltimore, MD (UMB). Support for this research was provided by a National Science Foundation (NSF) Growing Convergence Research (GCR) grant. The authors gratefully acknowledge this support. Any opinions, findings, and conclusions or recommendations expressed in this work are those of the author(s) and do not necessarily reflect those of NSF.

REFERENCES

[1] S. R. Carr, J. P. Cantor, A. S. Rao, T. V. Lakshman, J. E. Collins, and J. S. Friedberg, "Peritoneal perfusion with oxygenated perfluorocarbon augments systemic oxygenation," *Chest*, vol. 130, no. 2, pp. 402–411, 2006.

[2] A. W. Kirkpatrick, D. J. Roberts, J. De Waele, R. Jaeschke, M. L. Malbrain, B. De Keulenaer, J. Duchesne, M. Bjorck, A. Leppaniemi, J. C. Ejike *et al.*, "Intra-abdominal hypertension and the abdominal compartment syndrome: updated consensus definitions and clinical practice guidelines from the world society of the abdominal compartment syndrome," *Intensive care medicine*, vol. 39, no. 7, pp. 1190–1206, 2013.

[3] A. Regli, P. Pelosi, and M. L. Malbrain, "Ventilation in patients with intra-abdominal hypertension: what every critical care physician needs to know," *Annals of intensive care*, vol. 9, no. 1, pp. 1–19, 2019.

[4] A. R. Blaser, M. Björck, B. De Keulenaer, and A. Regli, "Abdominal compliance: a bench-to-bedside review," *Journal of Trauma and Acute Care Surgery*, vol. 78, no. 5, pp. 1044–1053, 2015.

[5] M. L. Malbrain, D. Chiumello, P. Pelosi, A. Wilmer, N. Brienza, V. Malcangi, D. Bihari, R. Innes, J. Cohen, P. Singer *et al.*, "Prevalence of intra-abdominal hypertension in critically ill patients: a multicentre epidemiological study," *Intensive care medicine*, vol. 30, no. 5, pp. 822–829, 2004.

[6] A. R. Blaser, A. Regli, B. De Keulenaer, E. J. Kimball, L. Starkopf, W. A. Davis, P. Greiffenstein, J. Starkopf *et al.*, "Incidence, risk factors, and outcomes of intra-abdominal hypertension in critically ill patients—a prospective multicenter study (iroi study)," *Critical care medicine*, vol. 47, no. 4, p. 535, 2019.

[7] A. B. Cresswell, W. Jassem, P. Srinivasan, A. A. Prachalias, E. Sizer, W. Burnal, G. Auzinger, P. Muiesan, M. Rela, N. D. Heaton *et al.*, "The effect of body position on compartmental intra-abdominal pressure following liver transplantation," *Annals of intensive care*, vol. 2, no. 1, pp. 1–10, 2012.

[8] P. Y. Durand, J. Chanliau, J. Gamberoni, D. Hestin, and M. Kessler, "Apd: clinical measurement of the maximal acceptable intraperitoneal volume," *Advances in peritoneal dialysis*, vol. 10, pp. 63–63, 1994.

[9] R. Scanziani, B. Dozio, I. Baragetti, and S. Maroni, "Intraperitoneal hydrostatic pressure and flow characteristics of peritoneal catheters in automated peritoneal dialysis," *Nephrology Dialysis Transplantation*, vol. 18, no. 11, pp. 2391–2398, 2003.

[10] B. De Keulenaer, J. De Waele, B. Powell, and M. Malbrain, "What is normal intra-abdominal pressure and how is it affected by positioning, body mass and positive end-expiratory pressure?" *Intensive care medicine*, vol. 35, no. 6, pp. 969–976, 2009.

[11] M. L. Malbrain, J. J. De Waele, A. W. Kirkpatrick *et al.*, "Intra-abdominal hypertension: definitions, monitoring, interpretation and management," *Best practice & research Clinical anaesthesiology*, vol. 27, no. 2, pp. 249–270, 2013.

[12] R. Chun, L. Baghirzada, C. Tiruta, and A. Kirkpatrick, "Measurement of intra-abdominal pressure in term pregnancy: a pilot study," *International journal of obstetric anesthesia*, vol. 21, no. 2, pp. 135–139, 2012.

[13] J. E. Varela, M. Hinojosa, and N. Nguyen, "Correlations between intra-abdominal pressure and obesity-related co-morbidities," *Surgery for Obesity and Related Diseases*, vol. 5, no. 5, pp. 524–528, 2009.

[14] F. Fuchs, M. Bruyere, M.-V. Senat, E. Purenne, D. Benhamou, and H. Fernandez, "Are standard intra-abdominal pressure values different during pregnancy?" *PLoS One*, vol. 8, no. 10, p. e77324, 2013.

[15] K. Verbeke, I. Casier, B. VanAcker, B. Dillemans, and J. Mulier, "Impact of laparoscopy on the abdominal compliance is determined by the duration of the pneumoperitoneum, the number of gravidity and the existence of a previous laparoscopy or laparotomy: 1ap9–3," *European Journal of Anaesthesiology— EJA*, vol. 27, no. 47, pp. 29–30, 2010.

[16] P.-Y. Durand, P. Balteau, J. Chanliau, and M. Kessler, "Optimization of fill volumes in automated peritoneal dialysis," *Peritoneal dialysis international*, vol. 20, no. 2_suppl, pp. 83–88, 2000.

[17] J. P. Mulier, B. Dillemans, M. Crombach, C. Missant, and A. Sels, "On the abdominal pressure volume relationship," *The Internet Journal of Anesthesiology*, vol. 21, no. 1, pp. 5221–5231, 2009.

[18] T. S. Papavramidis, N. A. Michalopoulos, G. Mistriotis, I. G. Pliakos, I. I. Kesisoglou, and S. T. Papavramidis, "Abdominal compliance, linearity between abdominal pressure and ascitic fluid volume," *Journal of Emergencies, Trauma and Shock*, vol. 4, no. 2, p. 194, 2011.

[19] A. Regli, B. L. De Keulenaer, B. Singh, L. E. Hockings, B. Noffsinger, and P. V. van Heerden, "The respiratory pressure—abdominal volume curve in a porcine model," *Intensive care medicine experimental*, vol. 5, no. 1, pp. 1–12, 2017.

[20] C. I. Castro and J. C. Briceno, "Perfluorocarbon-based oxygen carriers: review of products and trials," *Artificial organs*, vol. 34, no. 8, pp. 622–634, 2010.

[21] N. Legband, L. Hatoum, A. Thomas, C. Kreikemeier-Bower, D. Hostetler, K. Buesing, M. Borden, and B. Terry, "Peritoneal membrane oxygenation therapy for rats with acute respiratory distress syndrome," *Journal of medical devices*, vol. 10, no. 2, 2016.

[22] R. Okabe, T. F. Chen-Yoshikawa, Y. Yoneyama, Y. Yokoyama, S. Tanaka, A. Yoshizawa, W. L. Thompson, G. Kannan, E. Kobayashi, H. Date *et al.*, "Mammalian enteral ventilation ameliorates respiratory failure," *Med*, vol. 2, no. 6, pp. 773–783, 2021.

[23] N. Faithfull, J. Klein, H. Vanderzee, and P. Salt, "Whole body oxygenation using intraperitoneal perfusion of fluorocarbons," *British journal of anaesthesia*, vol. 56, no. 8, pp. 867–872, 1984.

[24] M. Doosthosseini, K. R. Aroom, M. Aroom, M. Culligan, W. Naselsky, C. Thamire, H. W. Haslach Jr, S. A. Roller, J. R. Hughen, J. S. Friedberg *et al.*, "Monitoring and control system development and experimental validation for a novel extrapulmonary respiratory support setup," *arXiv preprint arXiv:2107.02902*, 2021.